

# Mean Arteriolar Diameter Measured from Wide-Field Swept-Source OCT Angiography: A Highly Sensitive Indicator for Mean Arterial Pressure

Yuchen Li,<sup>1,\*</sup> Yuyao Qu,<sup>1,\*</sup> Hanze Zhang,<sup>1</sup> Yue Bian,<sup>1</sup> Langxuan Yuan,<sup>1</sup> Jingbo Hu,<sup>1</sup> Shengrui Xu,<sup>2,3</sup> Xiayu Xu, PhD,<sup>2,3</sup> Jianqin Lei, MD<sup>1</sup>

**Purpose:** To investigate the metrics of retinal arterioles and venules based on the en face images of the superficial retina using wide-field swept-source OCT angiography (SSOCTA) and assess their relationships with specific systemic parameters in a normal sample.

**Design:** Cross-sectional study.

**Participants:** Normal volunteers with no history of hypertension, diabetes, or significant eye diseases were recruited at the outpatient clinic of the First Affiliated Hospital of Xi'an Jiaotong University. Eligible eyes had a corrected visual acuity of 20/25 or better and an intraocular pressure (IOP) not exceeding 21 mmHg.

**Methods:** The SSOCTA scans of 24 × 20 mm in size were acquired from both eyes of each participant, along with measurements of axial length (AL), IOP, real-time mean arterial pressure (MAP), and body mass index (BMI). Retinal arterioles and venules were manually segmented and distinguished from the disc margin to their capillary junctions in the superficial retinal layer. Image processing and calculations were performed using ImageJ.

**Main Outcome Measurements:** The averaged caliber and fractal dimension of arteries and veins, as well as the arteriovenous ratio, were calculated from binarized vascular images. Generalized linear mixed models were used to test correlations between systemic parameters and these metrics.

**Results:** A total of 54 eyes from 44 participants were included after screening. Univariate analysis revealed a significant negative impact of MAP on averaged caliber of retinal artery ( $B = -0.003$ ,  $P = 0.004$ ) and averaged caliber of retinal vein (ACvein) ( $B = -0.002$ ,  $P = 0.045$ ), whereas age, sex, BMI, AL, and IOP showed no significant impact on these metrics. Variations among graders significantly influenced most metrics; however, real-time MAP continued to predict retinal arteriolar caliber after adjusting for graders ( $B = -0.002$ ,  $P = 0.03$ ).

**Conclusions:** The mean arteriolar diameter measured using wide-field SSOCTA could serve as a highly sensitive indicator of systemic vascular changes.

**Financial Disclosure(s):** Proprietary or commercial disclosure may be found in the Footnotes and Disclosures at the end of this article. *Ophthalmology Science* 2025;5:100679 © 2024 by the American Academy of Ophthalmology. This is an open access article under the CC BY-NC-ND license (<http://creativecommons.org/licenses/by-nc-nd/4.0/>).

The eye is a unique organ that provides noninvasive access to microcirculation. Retinal vascular parameters observed in fundus photography have been identified as biomarkers for predicting cardiovascular and cerebrovascular diseases. Narrowing of arterioles, for instance, has demonstrated prognostic value in the development of hypertension, as shown in studies such as the Rotterdam Study and the Blue Mountains Eye Study.<sup>1,2</sup> In these large cohort studies, retinopathy and decreases in arteriovenous ratio (AVR) were also reported as predictors of stroke risk.<sup>3,4</sup> Additionally, a previous meta-analysis found that a higher body mass index was independently associated with both retinal arteriolar narrowing and venular widening.<sup>5</sup> Of note, the association was also found in participants without diabetes or hypertension.<sup>6</sup>

These studies, however, relied primarily on color fundus photographs that capture only large vessels in the peripapillary area. The repeatability of vascular caliber measurements in these images is moderate, with an intergrader correlation coefficient of 0.79.<sup>7</sup> Compared to traditional fundus photography, OCT angiography (OCTA) offers significantly improved resolution and contrast for visualizing retinal microvasculature. This advancement facilitates enhanced digital image processing capabilities, enabling precise quantitative measurements. Previous studies have shown excellent repeatability in assessing retinal microvasculature using OCTA,<sup>8,9</sup> with intraclass correlation coefficients as high as 0.92 to 0.95 for superficial capillary measurements in 3 × 3 mm en face images.<sup>9</sup> However, typical OCTA-based measurements

usually encompass retinal capillaries, arterioles, and venules collectively, making it challenging to segment and calculate each vascular component separately.

Our prior research developed a fully automated arteriole–venule segmentation and differentiation method, AV-casNet, based on  $6 \times 6$  and  $3 \times 3$  mm en face OCTA images, allowing for more precise and convenient vascular calculations.<sup>10</sup> This method, however, was limited to displaying only the central macular or peripapillary areas, and it produced more segmentation errors when applied to other types of OCTA devices. Recently, a newer generation of swept-source OCT angiography (SSOCTA) has emerged, offering faster scanning speeds and much wider fields of view, reaching up to  $24 \times 20$  mm in a single scan.<sup>11</sup>

In this study, we segmented arterioles and venules from the  $24 \times 20$  mm SSOCTA en face images, tracing them from the largest trunks to the smallest branches, and evaluated the potential factors impacting vascular metrics in a sample of healthy individuals.

## Methods

### Data Collection

In this cross-sectional study, normal volunteers were recruited at the First Affiliated Hospital of Xi'an Jiaotong University from January to February 2023. Participants completed a brief questionnaire covering their medical and ocular history, height, and weight. During the same visit, the following examinations were performed: blood pressure (BP), best-corrected visual acuity, intraocular pressure (IOP), slit-lamp examination, axial length (AL) measurement, and OCTA (BM-400K; TowardPi Medical Technology Co. Ltd.) scans ( $24 \text{ mm} \times 20 \text{ mm}$ , centered on the macular, scanning frequency: 400 kHz, scanning laser wavelength: 1060 nm) for both eyes. Eligibility criteria included best-corrected visual acuity of 20/25 or better,  $\text{IOP} \leq 21 \text{ mmHg}$ , and clear refractive media. Participants were excluded if they had a history of diabetes, hypertension, glaucoma, uveitis, or retinal disease or if there were any notable pathological features on OCTA en face or B-scan images. The study was approved by the Institutional Review Board of the First Affiliated Hospital of Xi'an Jiaotong University and conducted in accordance with the ethical standards stated in the Declaration of Helsinki. Written informed consent was obtained from all participants.

### Image Processing

Only images meeting the following criteria were processed and analyzed: (1) signal strength  $\geq 7$ , (2) clear visibility of arterioles and venules across the entire image, and (3) absence of horizontal shifts due to motion artifacts (Fig 1). The en face images of the retinal superficial capillary plexus underwent 3 main steps in image processing. First, retinal vessels were manually labeled, extending from the disc margin to precapillary arterioles or postcapillary venules. The labeling was terminated at the point where vessels bifurcate into multiple smaller branches. Each vascular tree was assigned a unique color using ITK-Snap (version 3.8.0) with the disc area masked (Fig 2A). Three graders performed the labeling without repetition. In the second

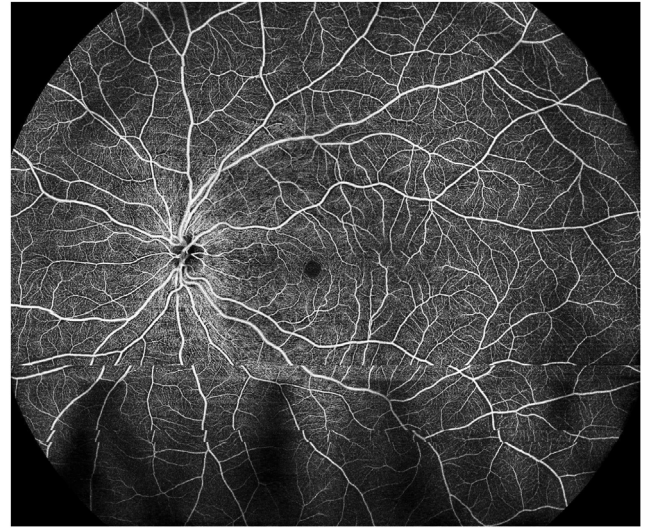


**Figure 1.** Wide-field en face image ( $24 \times 20$  mm) of the retinal superficial capillary plexus showing a distinct horizontal shift of the retinal vessels caused from motion artifact.

step, a retinal specialist (J.L.) distinguished arterioles from venules around the optic disc (Fig 2B) based on the following criteria: (1) the presence of a capillary-free zone associated with arteries; (2) arteries do not cross other arteries, and similarly, veins do not cross other veins; (3) vessels could be traced proximally and distally for identification; and (4) arteries and veins were arranged in an alternating pattern, with each vein draining capillary beds perfused by adjacent arteries.<sup>12</sup> Small vessels, such as cilioretinal arteries, were left unspecified. Using these 2 steps, each vascular tree was defined with cascading branches extending to precapillary arterioles or postcapillary venules (Fig 2C). Image processing was conducted at the Key Laboratory of Biomedical Information Engineering, Ministry of Education, Xi'an Jiaotong University, and the labeled images were prepared for future machine learning and automatic segmentation.

### Outcome Measurements

**Vessel Calibers.** The labeled arteries and veins were extracted separately, followed by binarization and skeletonization using ImageJ (version 1.54f) (Fig 2D–F). The averaged caliber of retinal arteries and veins, termed averaged caliber of retinal artery (ACartery) and averaged caliber of retinal vein (ACvein), was calculated using the following formula. The AVR was defined as  $\text{AVR} = \text{ACartery}/\text{ACvein}$ .

$$\text{AC} = \frac{\text{VD}}{\text{SVD}}$$

where AC is the averaged caliber; VD is the vessel density; and SVD is skeletonized vessel density.

**Fractal Dimensions.** The complexity of retinal arteries and veins was evaluated using fractal dimensions, termed FDartery and FDvein. The “Fractal Analysis” plugin in ImageJ, specifically the “FracLac” tool (version 2015Sep090313a9330), was used. The setup is displayed in Figure 3, and fractal dimensions were calculated automatically after scanning the binarized image of the retinal arteries or veins.

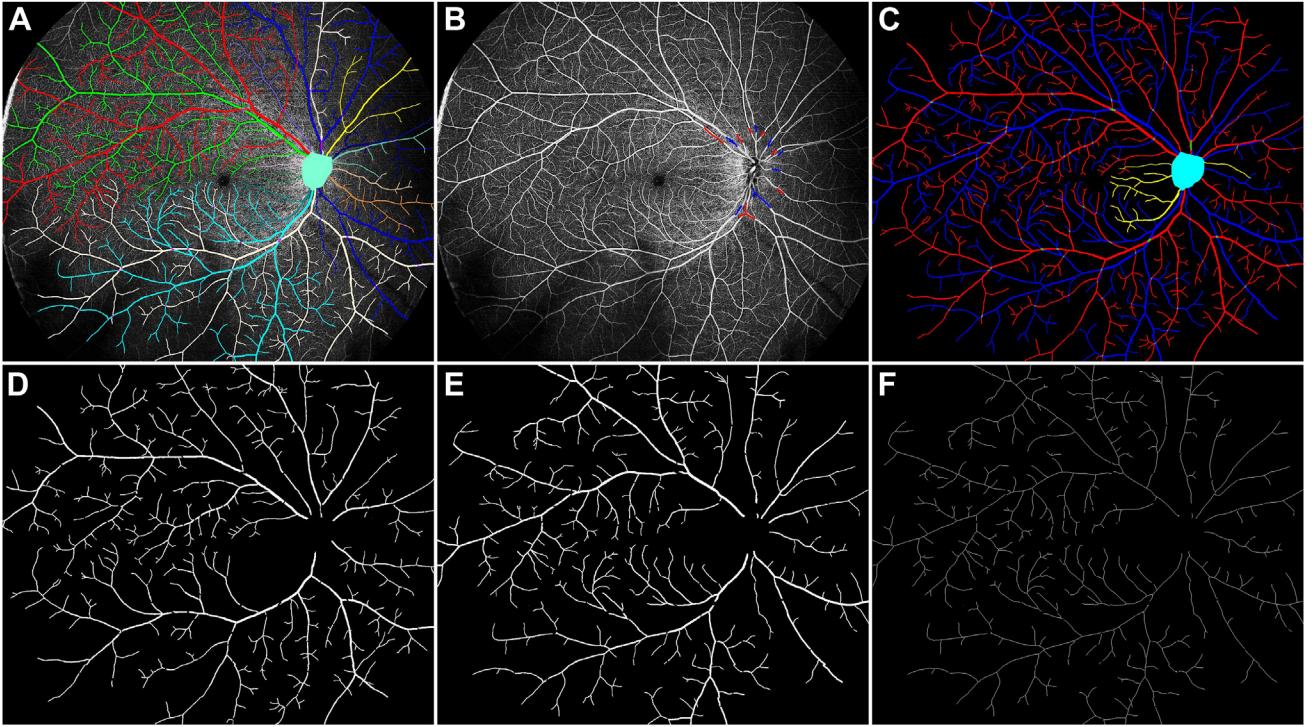


**Figure 2.** An example of the image process on the  $24 \times 20$  mm OCT angiography en face image. **A**, Manual segmentations of the retinal arterioles and venules with optic disc masked (each color represents a vessel branch). **B**, Labels of each major vessel branch as artery (red) or vein (blue) drawn by a retinal specialist. **C**, Distinctive segmentations of the retinal arteries and veins. Unspecified small branches were segmented in yellow. **D**, Binarized image of the retinal arterioles only. **E**, Binarized image of the retinal venules only. **F**, Skeletonized image of the retinal venules.

## Statistics

Because data from one or both eyes of a participant could be included, generalized linear mixed models were used to assess the impact of factors, such as age, gender, IOP, AL, mean arterial pressure (MAP), body mass index, and grader variations, on outcome measurements. For factors showing significant impact on univariate analysis, multivariate analysis was conducted to adjust for interactions. Statistical analyses were performed using SPSS (version 24; IBM Corp.), with a  $P$  value  $<0.05$  considered statistically significant.

## Results

Initially, images were collected from 156 eyes of 78 volunteers; all of whom were of Asian ethnicity. After a strict screening process to facilitate manual segmentation for future machine learning, a total of 54 eyes (27 right eyes) from 44 participants (11 males) were included in the study. A large proportion of images were excluded due to vascular discontinuity from motion artifact. The general demographics of the sample are presented in Table 1. Among the factors assessed, only MAP and IOP showed a normal distribution.

The mean values for ACartery, ACvein, AVR, FDartery, and FDvein were  $60.13 \pm 3.99$  ( $51.23$ – $75.31$ )  $\mu\text{m}$ ,  $65.57 \pm 4.22$  ( $56.76$ – $78.92$ )  $\mu\text{m}$ ,  $0.92 \pm 0.03$  ( $0.84$ – $0.98$ ),  $1.64 \pm 0.02$  ( $1.56$ – $1.68$ ), and  $1.62 \pm 0.02$  ( $1.54$ – $1.66$ ), respectively. The coefficients of variation for these metrics among normal eyes were 6.63%, 6.43%, 3.25%, 3.10%, and 1.41%, respectively.

Univariate analysis using generalized linear mixed models, as shown in Table 2, indicated a negative correlation between MAP and ACartery ( $B = -0.003$ ,  $P = 0.004$ ) as well as ACvein ( $B = -0.002$ ,  $P = 0.045$ ). Neither age nor AL significantly impacted these measurements. However, variations among graders did affect the outcome measurements. When Grader 3 was set as the reference, Grader 2 showed correlations with ACartery ( $B = 0.077$ ,  $P_{\text{vein}} [B = -0.071, P = 0.001]$ ), AVR ( $B = -0.024$ ,  $P = 0.003$ ), and FDartery ( $B = 0.031$ ,  $P_{\text{vein}} [B = 0.015, P = 0.001]$ ). Grader 1, in contrast, was only correlated with FDartery ( $B = 0.015$ ,  $P = 0.033$ ).

To adjust for grader variations, multivariate analyses were conducted, and the results are presented in Table 3. After adjustment, MAP remained a predictor of retinal arteriolar diameter ( $B = -0.002$ ,  $P = 0.03$ ).



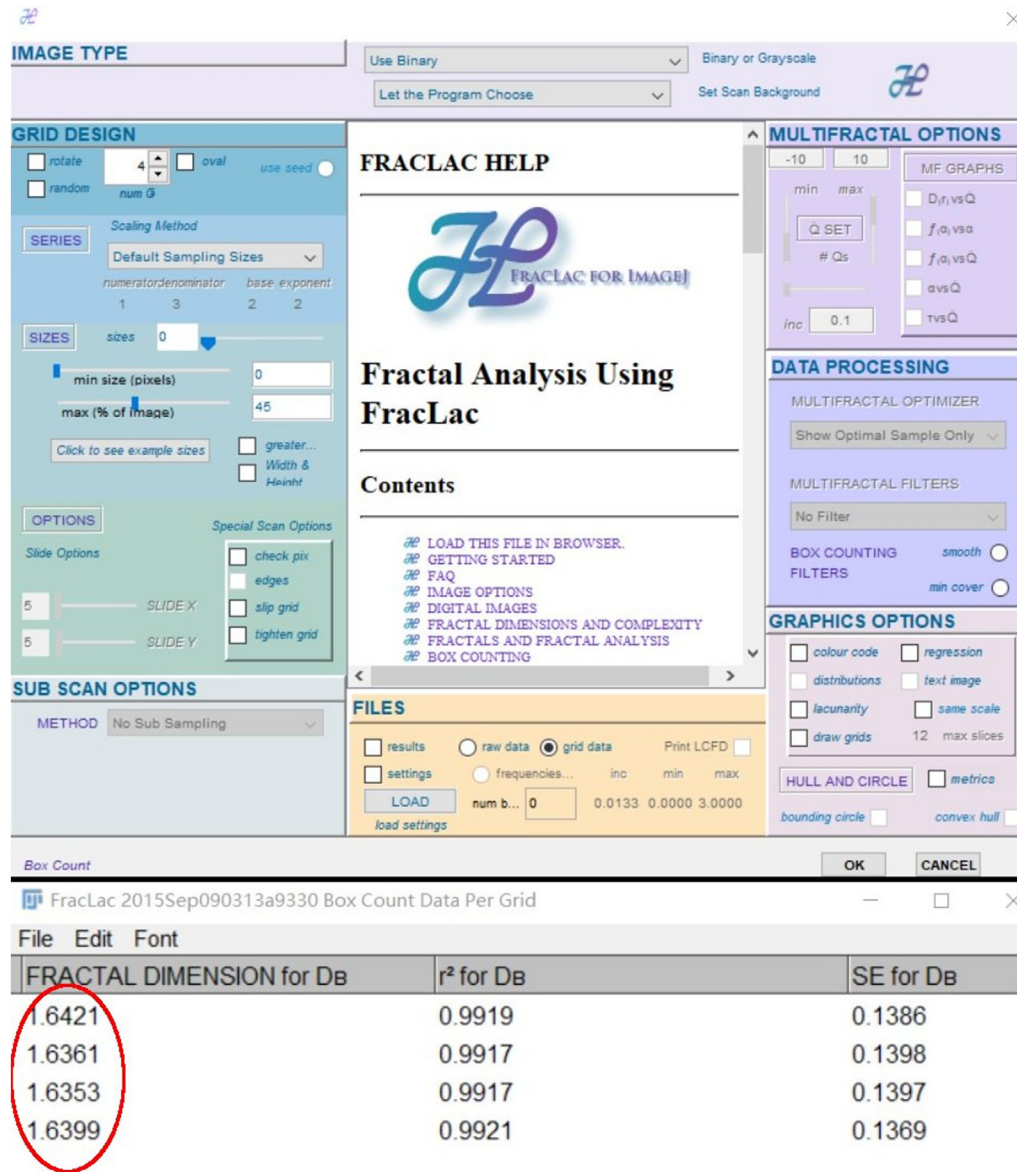


**Figure 3.** Upper part: The screenshot of the setups of the fractal analysis. Lower part: The results of the fractal dimension of retinal vessels in 4 different positions, and we used the mean value.

## Discussion

In this pioneering study of retinal arterioles and venules using wide-field SSOCTA, we found that retinal arteriolar caliber is capable of predicting real-time systolic BP, even within a small normal cohort. This finding suggests that retinal arteriolar diameter could serve as a remarkably sensitive metric for evaluating systemic vascular conditions. Additionally, this result supports the pressure-dependent nature of retinal arterial flow, aligning with the well-established Bayliss effect.<sup>13</sup>

Previous research has established similar associations; however, most of these studies were large, population-based investigations relying on color fundus photographs as the primary imaging modality. Prominent examples include the Atherosclerosis Risk in Communities<sup>7</sup> and Beaver Dam<sup>14</sup> studies, where arteriolar caliber was measured in a region 0.5 to 1 disc diameter from the optic disc, with vessels under 25  $\mu\text{m}$  excluded. Both human and animal experiments have indicated that arterioles with smaller diameters may exhibit heightened sensitivity to BP or hypoxia-induced diameter changes.<sup>15–17</sup> This phenomenon

Table 1. Demographics of the Sample

	Group		Frequency	Rate	
Eye		R	27	50%	
		L	27	50%	
Grader		1	19	35.2%	
		2	18	33.3%	
		3	17	31.5%	
	N	Min	Max	Means	SD
Age (yrs)	54	20	77	43	17
MAP (mmHg)	51	72	104	89	8
IOP (mmHg)	54	9.9	20.2	15.2	2.4
AL (mm)	54	21.68	27.64	24.05	1.50
BMI	52	14.2	30.6	18.1	2.6

AL = axial length; BMI = body mass index; IOP = intraocular pressure; MAP = mean arterial pressure; SD = standard deviation.

may explain the high sensitivity of our measurements, which included precapillary arterioles. Although advanced digital image processing has been developed to analyze whole retinal vessels based on color fundus photographs,<sup>18–20</sup> limitations remain because of innate drawbacks in fundus imaging, such as low contrast, uneven illumination, choroidal vascularization, light reflex, and background noise.<sup>21</sup>

In the past decade, OCTA has enabled a deeper understanding of fundus microvasculature by comparing signals across consecutive B-scans to reveal erythrocyte movement. This technique allows visualization of retinal arterioles, venules under 25  $\mu\text{m}$ , and even capillaries with high contrast. Moreover, measurements obtained from OCTA reflect blood flow within the lumen, excluding vessel wall

thickness, potentially contributing to our metrics' sensitivity to pressure changes. Studies using OCTA have shown that patients with hypertension experience significant decreases in deep retinal capillary plexus vessel density.<sup>22,23</sup> In another OCTA study including both healthy and hypertensive participants, Xu et al<sup>24</sup> measured peripapillary vessel calibers manually at certain points; however, neither arterial nor venous caliber was found to be correlated with MAP.

Although OCTA's built-in software typically quantifies all vessels in an en face image, recent studies have attempted to segment arterioles and venules separately.<sup>10,12</sup> Nonetheless, these studies generally have limited fields of view, preventing complete topological analysis of retinal vessels. Gao et al,<sup>25</sup> for example, presented a deep learning network for classifying arteries and veins in montaged OCTA images, but this approach was time-consuming and did not fully capture retinal arcades.

Our study stands out by using the newer generation SSOCTA, which allows us to capture a full view of retinal arteries and veins from root to branch in a single  $24 \times 20$  mm field of view, providing unique vessel metrics and identifying subtle changes under different BP conditions. Notably, our study revealed minimal variation in retinal artery and vein metrics within a normal cohort, with commonly reported confounding factors in OCTA studies, such as age and AL,<sup>26–28</sup> showing insignificant effects on our metrics. These strengths highlight the potential of wide-field SSOCTA in assessing systemic vascular diseases.

However, this study has limitations. First, the segmentations were performed manually, which is time consuming, and grader differences were evident. Despite this, arteriolar caliber remained significantly correlated

Table 2. Univariate Analysis Using Generalized Linear Mixed Model Showing the Correlations between Systemic/Ocular Parameters and Retinal Vascular Metrics

	Age	MAP	IOP	AL	BMI	Grader (2 vs. 3)
N	54	51	54	54	52	54
AC <sub>artery</sub>						
B	−0.001	−0.003	0.004	−0.008	−0.004	−0.077
P	0.291	0.004	0.271	0.167	0.330	0.000
AC <sub>vein</sub>						
B	−0.001	−0.002	0.003	−0.011	−0.001	−0.071
P	0.330	0.045	0.476	0.054	0.796	0.001
AVR						
B	0.000	−0.001	0.000	0.002	−0.002	−0.024
P	0.879	0.186	0.846	0.506	0.197	0.003
FD <sub>artery</sub>						
B	0.000	0.000	0.000	0.000	−0.001	0.031
P	0.919	0.337	0.904	0.939	0.663	0.000
FD <sub>vein</sub>						
B	0.000	0.000	−0.001	0.001	0.000	0.015
P	0.831	0.164	0.458	0.517	0.977	0.001

ACartery = averaged caliber of retinal artery; ACvein = averaged caliber of retinal vein; AL = axial length; AVR = arteriovenous ratio; BMI = body mass index; FD = fractal dimension; IOP = intraocular pressure; MAP = mean arterial pressure.

Table 3. Multivariate Analysis Using Generalized Linear Mixed Model Showing the Impact of MAP on the Caliber of Retinal Arterioles Adjusting for the Influence of Different Graders

	B	Standard Error	P	95% CI	
				Lower Boundary	Upper Boundary
MAP	−0.002	0.001	0.03	−0.004	−0.000
Grader 1	−0.017	0.019	0.388	−0.056	0.022
Grader 2	−0.064	0.021	0.004	−0.106	−0.022

CI = confidence interval; MAP = mean arterial pressure.

with MAP, even after adjusting for graders. These manual labels serve as ground truth data for future machine learning applications to enable automated segmentation.

## Footnotes and Disclosures

Originally received: August 6, 2024.

Final revision: November 8, 2024.

Accepted: December 12, 2024.

Available online: December 17, 2024. Manuscript no. XOPS-D-24-00281.

<sup>1</sup> Department of Ophthalmology, First Affiliated Hospital of Xi'an Jiaotong University, Xi'an, PR China.

<sup>2</sup> The Key Laboratory of Biomedical Information Engineering of Ministry of Education, School of Life Science and Technology, Xi'an Jiaotong University, Xi'an, PR China.

<sup>3</sup> Bioinspired Engineering and Biomechanics Center (BEBC), Xi'an Jiaotong University, Xi'an, PR China.

\*Y.L. and Y.Q. have contributed equally to this work and share first authorship.

Disclosure(s):

All authors have completed and submitted the ICMJE disclosures form.

The author(s) have made the following disclosure(s):

This work was supported in part by the National Natural Science Foundation of China under grant 82271098 and in part by the Shaanxi Natural Science Foundation of China under grant 2023-YBGY-233.

**HUMAN SUBJECTS:** Human subjects were included in this study. The study was approved by the Institutional Review Board of the First Affiliated Hospital of Xi'an Jiaotong University and conducted in accordance with the ethical standards stated in the Declaration of Helsinki. Written informed consent was obtained from all participants.

Second, the repeatability of measurements across graders or reproducibility across scans of the same individual was not assessed. Larger vessels, however, are likely less influenced by signal strength or shadow artifacts compared to smaller microvasculature. Lastly, the sample size in this preliminary study is relatively small, and neither age nor AL followed a normal distribution. A larger study population including cases with abnormal systemic vascular conditions is needed to identify additional biomarkers using wide-field OCTA.

In conclusion, this study represents the most extensive analysis to date of retinal arterioles and venules in a single wide-field image. We found a negative correlation between arteriolar caliber and MAP within a small normal sample, highlighting the sensitivity of this metric to BP variations and its potential application in assessing systemic vascular disorders.

No animal subjects were used in this study.

Author Contribution(s):

Conception and design: Lei, Xiayu Xu

Data collection: Lei, Li, Qu, Bian

Analysis and interpretation: Lei, Li, Qu, Zhang, Yuan, Hu, Shengrui Xu, Xiayu Xu

Obtained funding: N/A

Overall responsibility: Li, Qu

Abbreviations and Acronyms:

**ACartery** = averaged caliber of retinal artery; **ACvein** = averaged caliber of retinal vein; **AL** = axial length; **AVR** = arteriovenous ratio; **BP** = blood pressure; **IOP** = intraocular pressure; **MAP** = mean arterial pressure; **OCTA** = OCT angiography; **SSOCTA** = swept-source OCT angiography.

Keywords:

Mean arterial pressure, Retinal arterioles, Retinal venules, Segmentation, Wide-field swept-source OCT angiography.

Correspondence:

Jianqin Lei, MD, Department of Ophthalmology, First Affiliated Hospital of Xi'an Jiaotong University, 277# West Yan Ta Road, Xi'an 710061, Shaanxi, PR China. E-mail: [drleiq@163.com](mailto:drleiq@163.com); and Xiayu Xu, PhD, The Key Laboratory of Biomedical Information Engineering of Ministry of Education, School of Life Science and Technology, Xi'an Jiaotong University, 28# West Xian Ning Road, Xi'an 710049, Shaanxi, PR China. E-mail: [xiayuxu@xjtu.edu.cn](mailto:xiayuxu@xjtu.edu.cn).

## References

- Ikram MK, Witteman JC, Vingerling JR, et al. Retinal vessel diameters and risk of hypertension: the Rotterdam Study. *Am J Ophthalmol*. 2006;47:189–194.
- Smith W, Wang JJ, Wong TY, et al. Retinal arteriolar narrowing is associated with 5-year incident severe hypertension: the Blue Mountains Eye Study. *Hypertension*. 2004;44:442–447.
- Ikram MK, de Jong FJ, Bos MJ, et al. Retinal vessel diameters and risk of stroke: the Rotterdam Study. *Neurology*. 2006;66:1339–1343.
- Mitchell P, Wang JJ, Wong TY, et al. Retinal microvascular signs and risk of stroke and stroke mortality. *Neurology*. 2005;65:1005–1009.
- Boillot A, Zoungas S, Mitchell P, et al. Obesity and the microvasculature: a systematic review and meta-analysis. *PLoS One*. 2013;8:e52708.
- Wong TY, Duncan BB, Golden SH, et al. Associations between the metabolic syndrome and retinal microvascular signs: the Atherosclerosis Risk in Communities study. *Invest Ophthalmol Vis Sci*. 2004;45:2949–2954.
- Hubbard LD, Brothers RJ, King WN, et al. Methods for evaluation of retinal microvascular abnormalities associated with hypertension/sclerosis in the Atherosclerosis Risk in Communities Study. *Ophthalmology*. 1999;106:2269–2280.
- Coscas F, Sellam A, Glacet-Bernard A, et al. Normative data for vascular density in superficial and deep capillary plexuses

- of healthy adults assessed by optical coherence tomography angiography. *Invest Ophthalmol Vis Sci.* 2016;57:15–18793.
9. Lei J, Durbin MK, Shi Y, et al. Repeatability and reproducibility of superficial macular retinal vessel density measurements using optical coherence tomography angiography en face images. *JAMA Ophthalmol.* 2017;135:1092–1098.
  10. Xu X, Yang P, Wang H, et al. AV-casNet: fully automatic arteriole-venule segmentation and differentiation in OCT angiography. *IEEE Trans Med Imaging.* 2023;42:481–492.
  11. Zhao XY, Zhao Q, Wang CT, et al. Central and peripheral changes in retinal vein occlusion and fellow eyes in ultra-widefield optical coherence tomography angiography. *Invest Ophthalmol Vis Sci.* 2024;65:6.
  12. Abtahi M, Le D, Ebrahimi B, et al. An open-source deep learning network AVA-Net for arterial-venous area segmentation in optical coherence tomography angiography. *Commun Med.* 2023;3:54.
  13. Blum M, Bachmann K, Wintzer D, et al. Noninvasive measurement of the Bayliss effect in retinal autoregulation. *Graefes Arch Clin Exp Ophthalmol.* 1999;237:296–300.
  14. Wong TY, Knudtson MD, Klein R, et al. Computer-assisted measurement of retinal vessel diameters in the Beaver Dam Eye Study: methodology, correlation between eyes, and effect of refractive errors. *Ophthalmology.* 2004;111:1183–1190.
  15. Jeppesen P, Sanye-Hajari J, Bek T. Increased blood pressure induces a diameter response of retinal arterioles that increases with decreasing arteriolar diameter. *Invest Ophthalmol Vis Sci.* 2007;48:328–331.
  16. Skov JP, Aalkjaer C, Bek T. Differential effects of nitric oxide and cyclo-oxygenase inhibition on the diameter of porcine retinal vessels with different caliber during hypoxia ex vivo. *Exp Eye Res.* 2017;160:38–44.
  17. Skov Jensen P, Metz Mariendal Pedersen S, Aalkjaer C, Bek T. The vasodilating effects of insulin and lactate are increased in precapillary arterioles in the porcine retina ex vivo. *Acta Ophthalmol.* 2016;94:454–462.
  18. Huang C, Wang Z, Yuan G, et al. PKSEA-Net: a prior knowledge supervised edge-aware multi-task network for retinal arteriolar morphometry. *Comput Biol Med.* 2024;172:108–255.
  19. Fukutsu K, Saito M, Noda K, et al. A deep learning architecture for vascular area measurement in fundus images. *Ophthalmol Sci.* 2021;1:100004.
  20. Xu X, Wang R, Lv P, et al. Simultaneous arteriole and venule segmentation with domain-specific loss function on a new public database. *Biomed Opt Express.* 2018;9:3153–3166.
  21. van Overveld IM. Contrast, noise, and blur affect performance and appreciation of digital radiographs. *J Digit Imag.* 1995;8:168–179.
  22. Peng Q, Hu Y, Huang M, et al. Retinal neurovascular impairment in patients with essential hypertension: an optical coherence tomography angiography study. *Invest Ophthalmol Vis Sci.* 2020;61:42.
  23. Chua J, Chin CWL, Hong J, et al. Impact of hypertension on retinal capillary microvasculature using optical coherence tomographic angiography. *J Hypertens.* 2019;37:572–580.
  24. Xu Q, Sun H, Huang X, Qu Y. Retinal microvascular metrics in untreated essential hypertensives using optical coherence tomography angiography. *Graefes Arch Clin Exp Ophthalmol.* 2021;259:395–403.
  25. Gao M, Guo Y, Hormel TT, et al. A deep learning network for classifying arteries and veins in montaged Widefield OCT angiograms. *Ophthalmol Sci.* 2022;2:100–149.
  26. Shahlaee A, Samara WA, Hsu J, et al. In vivo assessment of macular vascular density in healthy human eyes using optical coherence tomography angiography. *Am J Ophthalmol.* 2016;165:39–46.
  27. Sampson DM, Gong P, An D, et al. Axial length variation impacts on superficial retinal vessel density and foveal avascular zone area measurements using optical coherence tomography angiography. *Invest Ophthalmol Vis Sci.* 2017;58:3065–3072.
  28. Leng Y, Tam EK, Falavarjani KG, Tsui I. Effect of age and myopia on retinal microvasculature. *Ophthalmic Surg Lasers Imaging Retina.* 2018;49:925–931.